Arabian Journal of Chemistry (2023) **16**, 104563

King Saud University

Arabian Journal of Chemistry

www.ksu.edu.sa
www.sciencedirect.com

ORIGINAL ARTICLE

Novel grasshopper protein/soy protein isolate/pullulan ternary blend with hesperidin derivative for antimicrobial edible film

Zisen Zhang [a], Changqing Fang [a,b,*], Wei Zhang [b], Wanqing Lei [b], Dong Wang [b], Xing Zhou [a,b,*]

[a] *School of Mechanical and Precision Instrument Engineering, Xi'an University of Technology, Xi'an, Shaanxi 710048, China*
[b] *Faculty of Printing, Packing Engineering and Digital Media Technology, Xi'an University of Technology, Xi'an, Shaanxi 710048, China*

Received 15 September 2022; accepted 5 January 2023
Available online 11 January 2023

KEYWORDS

Edible insects;
Locust (*Locusta migratoria*);
Grasshopper;
Insect protein;
Active packaging;
Methyl Hesperidin

Abstract As a green agricultural resource and a new alternative protein, edible insects have the potential to become an excellent source of biopolymer. In this study, a new ternary blend composites were formed based on the mixture of edible grasshopper protein and soybean protein isolates by adding pullulan (PUL). The combined effect of incorporation of antimicrobial agent methyl hesperidin (2.5 %, 5 %, 7.5 % and 10 %) was investigated. The addition of PUL can greatly improve the tensile strength of protein blend composites but has no positive impact on elongation at break. 5 % methyl hesperidin can further increase tensile strength to 7.36 MPa with no deterioration on elongation at break. The SEM and XRD results showed good compatibility between PUL and protein blend. The WVP and WCA results showed that the hydrophobicity of composites increased slightly. Moreover, thermal analysis presented that the thermal stabilities of composites were impaired. The increasing of methyl hesperidin content enhanced antibacterial activity against *E. coli* and *S. aureus* of ternary blend film, proving its application value as active packaging.

1. Introduction

Biopolymer are widely used in food, medicine and materials due to their biocompatibility and biodegradability. As an application scenario of biopolymer, edible film has become a major research direction in the field of food packaging since it was commercial in the 1960s because it helps to mitigate the increasingly serious plastic pollution problem. As one of the important raw materials of edible film, protein is mainly extracted from plants and animals. The most widely used and commercial animal-derived proteins are gelatin, which mainly extracted from pig skin (46 %), bovine hides (29.4 %), pig and cattle bones

* Corresponding authors at: School of Mechanical and Precision Instrument Engineering, Xi'an University of Technology, Xi'an, Shaanxi 710048, China.
E-mail addresses: fcqxaut@163.com (F. Changqing), zdxnlxaut@163.com (X. Zhou).

Peer review under responsibility of King Saud University.

Production and hosting by Elsevier

https://doi.org/10.1016/j.arabjc.2023.104563

(23.1 %) (Luo et al., 2022). This does not apply to Halal and Kosher consumers with religious taboos (Muslim and Jewish communities, making up about 23 % of global population) (Huang, et al., 2019). In addition, frequent outbreaks of livestock diseases (such as bovine spongiform encephalopathy, foot-and-mouth disease and swine influenzas) have raised concerns about the safety of consumption of such products (Lv, et al., 2019). These restrictions on use sparked a strong interest in finding alternatives.

As the largest animal group on earth, insects are known to have up to 5.5 million species, which is the largest untapped biological resource in nature. The use of insect-derived proteins as biopolymer materials mainly derived from insect secretions which can be traced back to 3000 BCE in China, where silk was used as textile materials for clothing (Reddy et al., 2021). Entomophagy, the practice of eating insects, has developed into a cuisine culture in many regions. Nowadays more than 2000 species of edible insects are consumed by more than 2.5 billion people because of their rich nutritional content and good taste. Protein is the most abundant nutrient component of edible insects, up to 750 g/kg on a dry matter basis, higher than beans (23.5 % of protein), lentils (26.7 %) or soybean (41.1 %) (Haber et al., 2019, Zielińska et al., 2015). Compared with traditional animal derived protein, edible insects are a more environmental-friendly and sustainable agricultural resource. In addition to its high nutrient protein and minerals and easy to digest properties, breeding insects is a green and circular economy, which has higher feed conversion efficiency and requires less land and water and emitted fewer greenhouse gases (Govorushko et al. 2019). Moreover, lower artificial breeding technology and costs make it easy to promote employment among the poor. The global market for edible insects is forecast to exceed $6 billion by 2030 (Anankware et al., 2021). At present, edible insects are mainly used as nutrient food and feed supplements. The latest researches revolve around these two topics. However, as a widely available and low-cost protein, the huge potential of edible insect proteins as feasible sources of biopolymer seems to be overlooked and relevant research was rare. Barbi et al. (2019) and Nuvoli et al. (2021) both tentatively produced the edible film with protein extracted from black soldier fly (*Hermetia illucens*) prepupae using solvent casting method.

Grasshopper, as a troublesome pest in global agriculture, have a long history of being used as food in many regions. Apart from the advantages of high protein content, short life cycles and fast growth rates (Clarkson et al., 2018), recent study reported that farming agricultural pests can be beneficial for protecting crops. In previous studies we explored the optimal film-forming conditions of grasshopper (*Locusta migratoria*) protein and studied the effects of soybean protein isolate and xylose as cross-linking agents on the performance of the composite protein film (Zhang et al., 2022a, Zhang et al., 2022b). It is expected to introduce a polysaccharide as a third phase to further improve the physicochemical properties of the edible film as antimicrobial packaging.

As a common water-soluble polysaccharide, pullulan (PUL) is developed through microbial fermentation with a similar structure to starch (Tabasum et al., 2018). It can be regarded as an intermediate between amylase and dextran structures due to existence of both α-(1 → 4) and α-(1 → 6) linkages in a single compound (Singh, et al., 2015). Its excellent barrier properties (highly impermeable to oil and oxygen), biocompatibility and biodegradability make it widely used in food packaging (Khanzadi et al., 2015). Previous studies showed that PUL has good compatibility with proteins from common sources (zein and mung bean protein) and significantly improved mechanical and barrier properties (Amjadi, et al., 2022, Haghighatpanah, et al., 2022).

Citrus species is one of the most important fruit varieties in the world, 70 % of which is used to make juice. The production of juice produces peel waste equal to about 50 % of the weight of the fruit, which is an excellent source of phenolic compounds. One of the flavonoids in the waste, hesperidin, was reported to have good antibacterial and antioxidant activity (Wang et al., 2021). Methyl hesperidin (MH) is the methylated derivative of hesperidin with better water solubility and bioavailability (Pinho-Ribeiro et al., 2015).

Therefore, a new GP/SPI/PUL ternary blend with MH was prepared in this study. The effect of PUL as a new third phase on GP/SPI protein blend was studied. Furthermore, MH was added in film as antimicrobial agent to evaluate its antimicrobial activity. The physicochemical properties of this new ternary antimicrobial film were characterized.

2. Materials and method

2.1. Materials

Frozen adult grasshoppers (*Locusta migratoria*) were purchased from a farm in Xi'an (Shannxi, China). SPI was purchased from Cool Chemical Science and Technology Co., ltd. (Beijing, China). D-xylose ((98 %, Mw ∼ 150.13) was purchased from Macklin Biochemical Co., ltd. (Shanghai, China). PUL was purchased from Hefei Bomei Biotechnology Co., ltd. (Hefei, China). MH was purchased from Xi'an Yunyue Biotechnology Co., ltd. (Xi'an, China).

2.2. Protein extraction

GP were extracted in the same way as described in our previous study (Zhang et al., 2022a, 2022b).

2.3. Film preparation

6 % GP/SPI/PUL blend were dissolved in deionized water with 45 % (w/w) glycerol added. The ratio of GP/SPI blend to PUL was set at 100/0 (control group), 80/20, 75/25 and 70/30. Before the final blend of three phases, protein blend and PUL were dissolved in deionized water separately and stirred for 40 min. Protein solution was prepared according to GP/SPI (7/3) with 10 % (w/w) xylose added at 80 ℃. After three phases were completely mixed, MH (2.5 %, 5 %, 7.5 %, 10 %) was added and kept to stir for 40 min at 40 ℃. The solution was cast in PTFE molds (8 × 8 cm) and dried at 50 °C for 24 h. All samples were labeled as control, PUL20, PUL25, PUL30, MH2.5, MH5, MH7.5, MH10 in above order, respectively.

2.4. Film characterization

2.4.1. Scanning electron microscope (SEM)

After soaking in liquid nitrogen, the fractured sections of samples were sprayed with gold and then put into an equipment (Jeol, JSM-6700, Japan) to observe the morphology and structure, setting the accelerating voltage at 3 kV.

2.4.2. Fourier transform infrared spectroscopy (FTIR)

Attenuated total reflectance-Fourier transform infrared (ATR-FTIR) spectrophotometer was used to scan film samples with the range at 500 ~ 4000 cm^{-1} wavenumber. (Vetex 70v, Bruker, Germany).

2.4.3. X-ray diffraction (XRD)

Ternary composites were analyzed by X-ray diffractometer (Shimadzu, XRD-7000, Japan) from 5° to 40° at 4°/min with Cu Kα source at 40 kV and 40 mA.

2.4.4. Mechanical properties

Film samples (75 × 15 mm) were tested with load cell of 500 N at a speed of 20 mm/min using Electronic Strength Tester (C610M, Labthink, China) according to the ASTM-D882 with modifications.

2.4.5. Differential scanning calorimeter (DSC)

DSC was tested by an instrument (DSC 200 F3 Maia®, NETZSCH, Germany). with the temperature range set at 0 ℃ to 200 ℃ by 10 ℃/min. All samples were heated from 30 ℃ to 100 ℃ with 10 ℃/min, kept for 1 min at 100 °C to eliminate thermal history before test.

2.4.6. Thermogravimetric analysis (TGA)

TGA was tested by an instrument (TG 209 F3 Tarsus®, NETZSCH, Germany), with the temperature range set at 30 ℃ to 550 ℃ and heat/cooling rate at 30 mL/min in nitrogen atmosphere.

2.4.7. Water vapor permeability (WVP)

WVP was tested by an instrument (PERME^{TM}W3/060, Labthink, China) whose test environment was set to 25 ℃ and 50 % RH (relative humidity). The machine automatically calculated the WVP value according to the following equation by measuring mass change.

$$WVP = (\Delta m \cdot X)/(A \cdot \Delta t \cdot \Delta P)$$

△m: mass change X: film thickness (mm) A: effective film area (m^2).

2.4.8. Water contact angle (WCA)

WCA was tested using a contact angle measurement instrument (OCA 20, Dataphysics, Germany) based on the sessile-drop method. Five different sites were selected on a flat sample surface and drop 2 μL of deionized water each time.

2.4.9. Viscosity

The viscosity of film solution was tested by viscometer (DV-Ⅱ+ Pro, Brookfield, USA) at different rpm.

2.4.10. Antimicrobial activity

The bacteriostatic test of Gram-positive *S. aureus* (ATCC 6538) and Gram-negative *E. coli* (ATCC 25922) was carried out using inhibition zone method. Sample PUL25 was selected as control group named as MH0. The sterilized circular sample (12 mm diameter) was placed on the beef extract peptone medium coated with 200 μL bacterial suspension (~10^6 CFU/mL). All samples were incubated at 37 ℃ and 70 % RH for 24 h and taken out to measure the diameter of inhibition zone.

3. Results and discussion

3.1. SEM

Cross-sectional images of all samples are presented in Fig. 1**.** In Fig. 1**(a)**, control group showed no obvious phase separation structure except creases and insoluble particles, indicating good compatibility between the two proteins. When PUL added as third phase, a typical morphology sea-island structure emerged, which looked more like a binary blend system. PUL was uniformly distributed in protein blend as a dispersed phase. With the increase of PUL content, it is observed that the size of dispersed phase also increased, and the aspect ratio of the dispersed phase became larger, from nearly round to rod. Saeb et al. (2012) also found the droplet size increased to some extent by increasing the weight content of minor phase. The addition of MH acted as a compatibilizer at the interface, reducing the interfacial tension and refining the dispersed phase (Moradi et al., 2020, Shariatpanahi, et al., 2003), and the bonds between dispersed phases were closer and the intervals were smaller. The size of dispersed phase was influenced by many factors, including viscosity, shear force and temperature. Sui et al. (2019) pointed out that high shear force was effective to decrease dispersed phase size. Rastin et al. (2014) got the conclusion that average viscosity or elasticity ratio of dispersed phase to matrix phase determined the size of droplets.

3.2. FTIR

The infrared absorption spectra of ternary blend are shown in Fig. 2**(a)** and **(b).** Amide bond is the characteristic structure of protein as the connecting unit after dehydration and condensation of amino acids. The C═O and C—N stretching vibration at ~ 1627 cm^{-1}, N—H bending at ~ 1558 cm^{-1}, and N—H in-plane bending with C—N stretching vibration at ~ 1200–145 0 cm^{-1} represented amide I, amide II and amide III, respectively (Ramos et al., 2013). The vibration intensity of C═O bond in amide I represented number of disordered conformation and amide II reflected the changes in the hydrogen bonds around the peptide chains (Li, et al., 2020, Omrani Fard, et al., 2020). The intensity of amide I and amide II both decreased indicated that hydroxyl groups in PUL and amino groups in protein blend were consumed, confirming successful crosslink between PUL and protein blend through Maillard reaction (Khadidja et al., 2017). A new peak in the ternary blend at ~ 1320 cm^{-1} after PUL was added, corresponding to –OH bending vibration (Tong et al., 2008). This suggested that PUL interacted with proteins to form hydrogen bonds, which contribute to the formation of dense network (Yang et al., 2020). The three-dimensional structure of polymer networks is formed by crosslinking one-dimensional polymer chains, which can form two types of crosslinks. Hydrogen and ionic bonds are usually driven by thermal fluctuations to form dynamic networks, while covalent bonds form permanent static networks (Katashima, 2021). During the heating process, conformational changes occurred first after protein denaturation. Then the interchain disulfide bonds formed after SH groups are exposed, and ultimate crosslink occurred interchain isopeptide to form a three-dimensional spatial network (Azeredo, et al., 2016, Gao et al., 2001). After the PUL was added, it was connected with the protein through the Maillard reaction to form a more powerful tridimensional network. The three peaks at ~ 755 cm^{-1}, 850 cm^{-1} and ~ 921 cm^{-1} belong to α-(1,4) glycosidic bonds, α-glucopyranoside units and α-(1,6) glycosidic bonds in PUL (Aceituno-Medina et al., 2013), of which the former was only shown in PUL20, while the latter two overlapped with the vibration peaks (C—C vibrations) induced by glycerol. (Ciannamea et al., 2014). The C—O stretching at ~ 1045 cm^{-1} was still from glycerol. The two peaks at ~ 2850 and ~ 2925 cm^{-1} belonged to

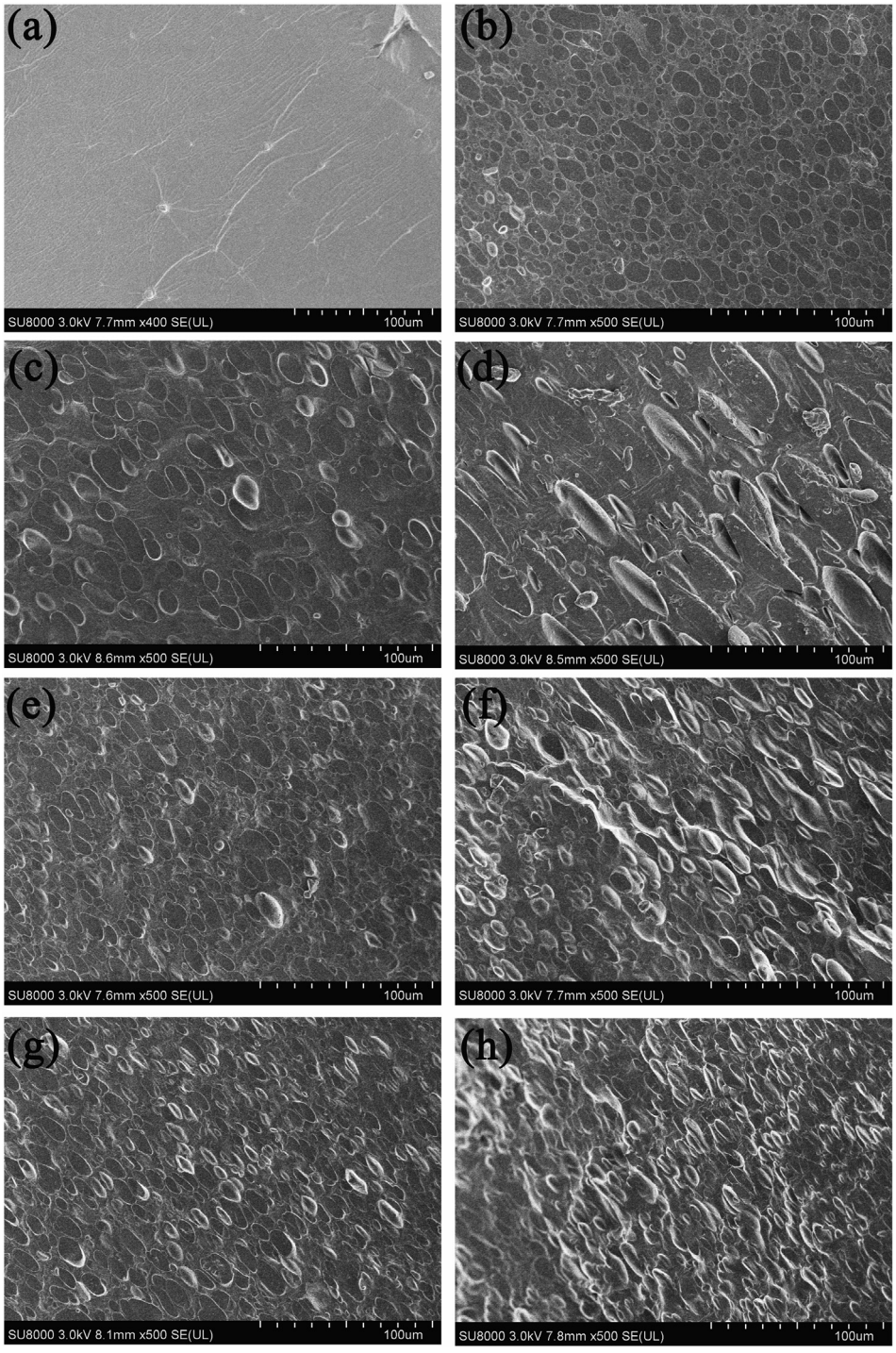

Fig. 1 Cross-section SEM images for ternary blend films (a) control (b) PUL20 (c) PUL25 (d) PUL30 (e) MH2.5 (f) MH5 (g) MH7.5 (h) MH10.

C—H stretching (Cao et al., 2018). The O—H stretching at ~ 3275 cm^{-1} from PUL overlapped with the N—H stretching from amide A in the same region and both affected by the inter-molecular/intra-molecular hydrogen bonds (Wu, et al., 2013). The peak at ~ 1107 cm^{-1} was intensified after PUL added ascribing to C—O bond at the C_4 position of a glucose residue from PUL overlapping with C—O stretching at C_2 from glycerol (Ciannamea et al., 2014, Xiao, et al., 2015).

3.3. XRD

According to previous studies (Haghighatpanah et al., 2020, Karim et al., 2009), PUL has a distinct characteristic peak at ~ 20°, corresponding to a d-spacing of 4.52°, representing its amorphous structure. The control group also had characteristic peaks at ~ 20° corresponding to the internal β-sheet structures of protein blends (Xia et al., 2016), as shown in

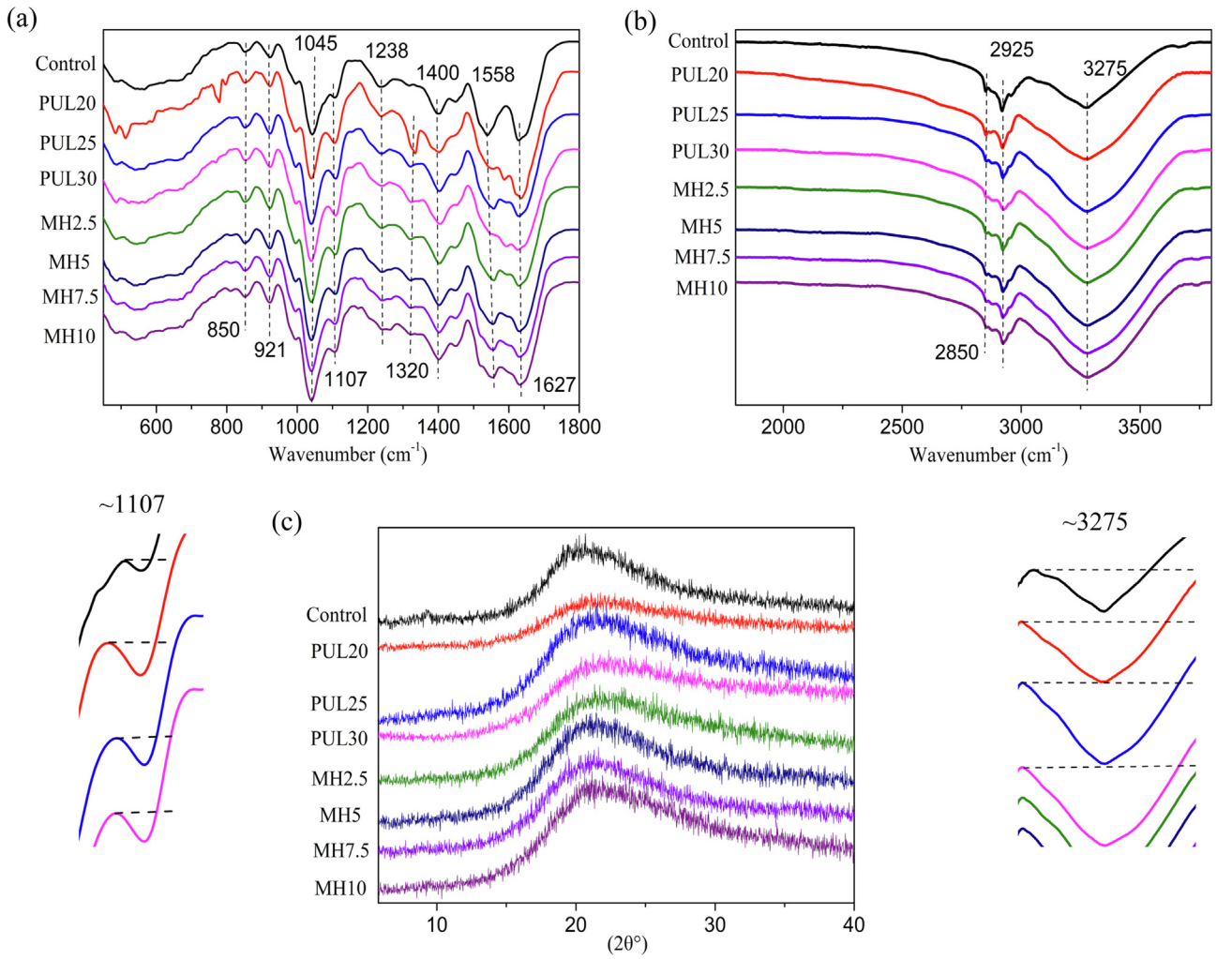

Fig. 2 ATR-FTIR spectra and XRD patterns of ternary blend films.

Fig. 2**(c)**. The decreased intensity of peak in PUL20 and PUL30 represented decreased crystallinity, indicating the intramolecular connection and the original ordered crystal structure were destroyed to some extent (Ahmed et al., 2020, Vinodhini et al., 2017). The XRD pattern changed little before and after MH addition, indicating that the interaction between MH and substrate may occur in the amorphous region without affecting the ordered crystal structure (Moghadam, et al., 2020). Zhang et al., (2020) observed that excessive cinnamaldehyde reduced the crystallinity of polymer due to the agglomeration and consuming space. Narasagoudr et al., (2020) found that 0.6 % rutin added in film increased crystallinity. Combined with above XRD results, it is suggested that the addition amounts of phenolic compounds should be controlled within a small scale in order not to reduce the crystallinity of materials.

3.4. Mechanical properties

The data of TS and EAB is presented in Fig. 3**.** When PUL is one of the components of blend film, it is not easy to increase TS substantially while keeping EAB basically stable or even growing. Especially when mixed with other polysaccharides, the TS of blend film usually increased, but EAB decreased significantly and not more than 6 %. Wu et al. (2013) reported the result that TS of chitosan/PUL blend increased from 48.8 MPa to 61.5 Mpa but EAB decreased from 19.2 % to 2.78 %. Prasad et al. (2008) reported the result that TS of hydroxypropyl methylcellulose/PUL blend increased from 35.51 MPa to 41.42 MPa and EAB decreased from 15.75 % to 5.55 %. Lian et al. (2020) suggested that the decrease of EAB was related to the fact that the polysaccharide broke the hydrogen bonds in the matrix and restricted its fluidity of the molecular chain as they observed both decrease in TS and EAB after PUL blended with chitosan. In this study, the addition of PUL significantly improved the TS of GP/SPI composite film while the 25 % PUL content increased most from 3.4 MPa to 7.0 MPa. This result was related to the dense three-dimensional network formed from the Maillard reaction between PUL and protein matrix (Qian et al., 2022). The arrangement and density of intermolecular and intramolecular interactions within the crosslinked network were closely related to the structure of polymer, thus determining the mechanical properties of the film (Al-Hassan et al., 2012). The effect of 2.5 % MH on blend film is similar to plasticizer, increasing EAB and decreasing TS. The plasticizer effect of the addition of phenolic compounds into biopolymers were often

reported in previous studies, such as mango peel extract combined with pectin (Ribeiro et al., 2021). The best mechanical properties were obtained with 5 % MH content: TS increased to 7.36 MPa and EAB stabilized at 38 %. Phenolic compound can crosslink with proteins through hydrogen bonds to form stronger interaction relationships and dense networks (Han et al., 2018). Prodpran et al. (2012) reported that phenolic compound can crosslinked with amino groups in proteins after being oxidized into quinone under alkaline conditions. Friesen et al. (2015) further summarized three ways on phenolic–protein interactions: (1) orthoquinone reacts with another quinone to form a dimer; (2) orthoquinone reacts with the amino side group in peptide; (3) orthoquinone reacts with another orthoquinone to form a dimer and cross link two chains together. Mathew et al. (2007) reported that polysaccharide-polysaccharide crosslinking reactions could also occur between phenolic compound and polysaccharides via free radical mediated cross linking, esterification with the hydroxyl groups and quinone-mediated reactions. Moreover, the finer dispersion phase with the addition of MH brought larger interfacial area, which allows the material to absorb more energy before fracture (Moradi et al., 2020). Good compatibility also improved the interfacial adhesion between phase components and formed a denser phase structure to strengthen mechanical properties of the film (Ren et al., 2009). The TS and EAB of 10 % MH samples were both lower than the PUL25, which was caused by the agglomeration of MH particles leading to stress concentration (McKay et al., 2021).

3.5. Thermal properties

The obvious endothermic peak appeared on the DSC curve after mixed with PUL, corresponding to the melting point (T_m) of ternary blend film, as shown in Fig. 4**(a).** The thermal stability data was listed in Table 1. Intermolecular forces, molecular symmetry, and conformational degree of free volume of a molecule played a major role in affecting the T_m (Hassannia-Kolaee et al., 2016). Increasing the ratio of PUL in ternary blend film from 20 % to 30 % led T_m value to increase from 180 ℃ to 190 ℃. Jia et al. (2020) observed same tendency and attributed it to the interactions between amino and carboxyl groups of protein and hydroxyl group of PUL. The result of decrease in T_m after MH added was related to the plasticizer function of MH mentioned earlier. MH reduced the energy required for melting by increasing the mobility of molecular chains and limiting intermolecular interactions (Yang et al., 2020). Moreover, MH could interfere with the ordered arrangement of polymer chains and increase spacing between them (Mohammadi et al., 2020). Ahmed et al. (2016) also pointed out that small plasticizer molecules affected the T_m by localizing at the crystalline and amorphous interfaces. The reduction of glass transition temperature (T_g) caused by MH addition was also closely bound up with this plasticizer effect.

As a neutral polysaccharide, PUL has better thermal stability than charged polysaccharide (Zhu et al., 2014). The T_{10} (Temperature of weight loss at 10 %) decreased significantly after PUL was added, indicating faster decomposition speed than control group. The T_{10} decreased further with the addition of MH in ternary blend. Moreover, the T_{10} continue to decrease with the increase in the amount of MH. The initial mass loss here is associated with evaporation of water vapor absorbed by the film and loss of low molecular weight compounds (He et al., 2019). The films with MH were more hygroscopic, thus degrading faster than control group. The most part of film degradation occurred between 180 ℃ and 400 ℃. In this temperature interval, glycerol and lower molecular weight protein were first lost, and then the main chains of proteins and PUL began to degrade (Qin et al., 2019, Wu, et al., 2020). T_{50} (Temperature of weight loss at 50 %) can be approximated to the temperature of maximum decomposition rate. The T_{50} of all samples were stabilized between 300 ℃ and 310 ℃, in other words, the degradation temperature of main polymer chain of all samples tended to be close, indicating that the modification had no effect on main polymer chain backbone. In the end, more than 23 % of the residual mass was left due to the high content of incombustible minerals and impurities in films. (Roy, 2021).

3.6. WVP

The WVP of pure PUL sample was 1.05×10^{-11} (g/cm·s·Pa), lower than the control group, as shown in Fig. 5**(a)**. After incorporation of PUL, the WVP of PUL25 and PUL30 decreased slightly due to the formed crosslinked network mentioned before. With the further addition of MH, WVP began to decrease when MH supplemental level was more than 5 %. The sugars moieties of MH can form hydrogen bonds with the free water retained by film and the substrate itself to produce a denser structure, thus reducing the mobility of

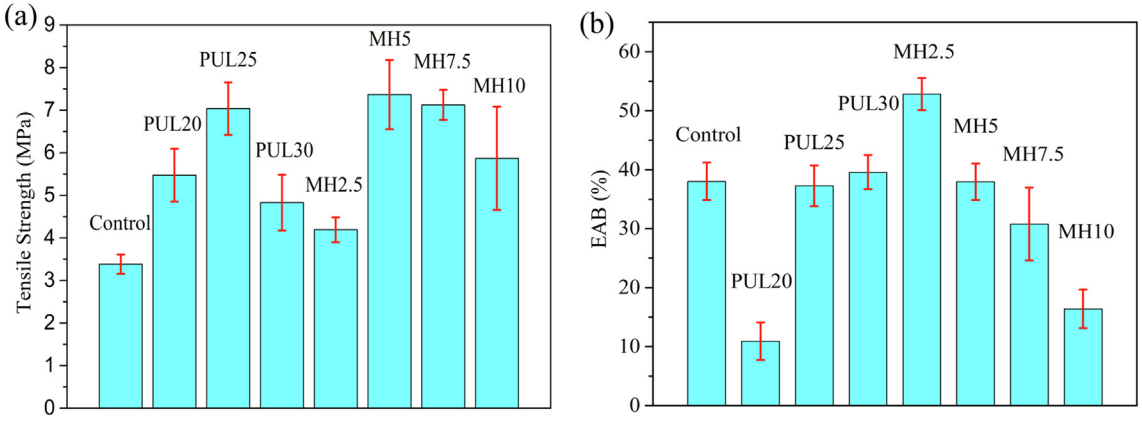

Fig. 3 Mechanical properties of ternary blend films.

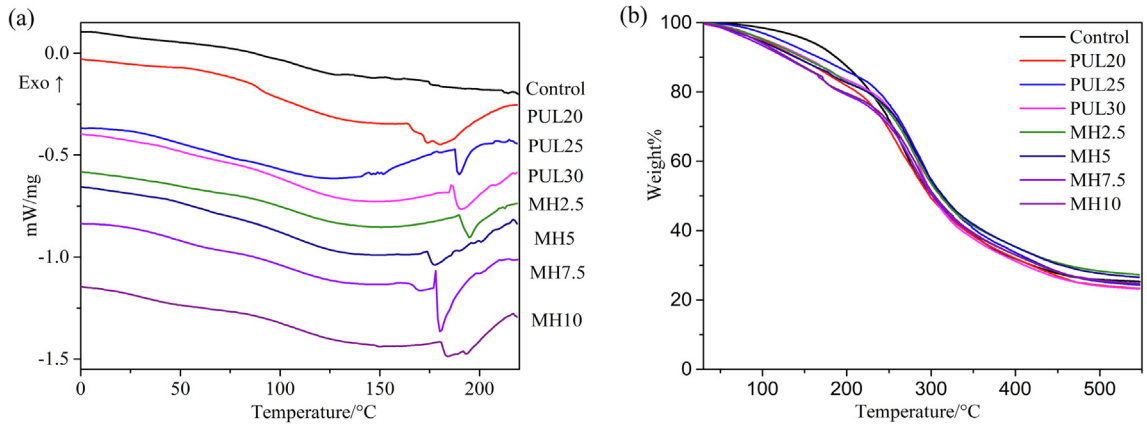

Fig. 4 DSC and TGA curves of ternary blend films.

Table 1 Thermal stability data for prepared films.

Samples	T_g (°C)	T_m (°C)	T_{10} (°C)	T_{50} (°C)	Mass loss (%)
Control	105.5		187.3	301.8	25.3
PUL20	92.4	179.9	140.2	298.3	23.3
PUL25	85.3	189.6	166.4	312.3	24.3
PUL30	95.1	190.8	150.7	301.8	23.2
MH2.5	103.1	194.9	147.5	310.9	27.3
MH5	103.3	177.3	139.3	313.9	26.5
MH7.5	94.2	180.2	126.8	301.5	24.7
MH10	93.5	184.3	129.3	304.2	24.6

water molecules in film to decrease WVP. (Friesen et al., 2015). However, there is no consistent effect of phenolic compounds on the WVP of packaging film. Haghighi et al., (2019) found five different types of 1 % essential oil all increased WVP of chitosan–gelatin films because the uneven structure caused by bubbles and oil droplets impaired the intermolecular forces and led to an open structure that facilitated the passage of water molecules. Shojaee-Aliabadi et al., (2013) added *Satureja hortensis* essential oil decreasing WVP of κ-carrageenan-based films significantly because hydrophobic dispersed phase could increase the tortuosity factor. Mathew et al., (2007) reported the incorporation of ferulic acid improved crosslinking degree and resulted in a better organized network to decrease WVP. Alexandre et al., (2016) found that ginger essential oils had no obvious effect on the WVP of gelatin-based film because they occupied the low part in dispersed systems. Hosseini et al., (2015) mentioned that the proportion of hydrophilic and hydrophobic components of film determined the WVP. These widely divergent results suggested that substrate type, polarity, morphology and amount of phenolic compound could affect their interaction, thus influencing the WVP.

3.7. WCA

The WCA of ternary blend films were shown in Fig. 5**(b).** According to previous studies (Lee et al., 2019, Zhao et al., 2019), the WCA of PUL films was between 50° and 60°, larger than the control group. After blending with PUL, the maximum WCA of film was increased from 29° to 37.6°. The crosslinking of proteins with polysaccharides depleted hydrophilic groups such as hydroxyl and amino groups forming a denser structure, resulting in the improvement of WCA (Qin, et al., 2020). The subsequent addition of MH did not significantly improve the WCA of film, and WCA was still not more than 40°, presenting a hydrophilic nature. Actually, the physical and chemical properties (surface energy and roughness) of material surface had a greater impact on the WCA, and many work to greatly improve the surface hydrophobicity was via surface treatment. The classical Wenzel Model showed that the increase of roughness can make the hydrophilic surface ($\theta < 90°$) more hydrophilic and the hydrophobic surface (θ greater than 90°) more hydrophobic (Quéré, 2008). Hurwitz et al. (2010) proved that the presence of divalent cations on film surface resulted in better hydrophilicity. Thus, for hydrophilic substrates like we used in this paper, it may be a good idea to improve WCA greatly by regulating the surface properties of film.

3.8. Viscosity

Several factors could determine the viscosity of solutions, such as impregnation properties, size and structure of solute molecules (Wu et al., 2011). The protein blend of the control group had a very low viscosity due to its effective volume was close to the volume of protein chains (Tong et al., 2022). It was observed from Fig. 6 that the overall viscosity of the film-

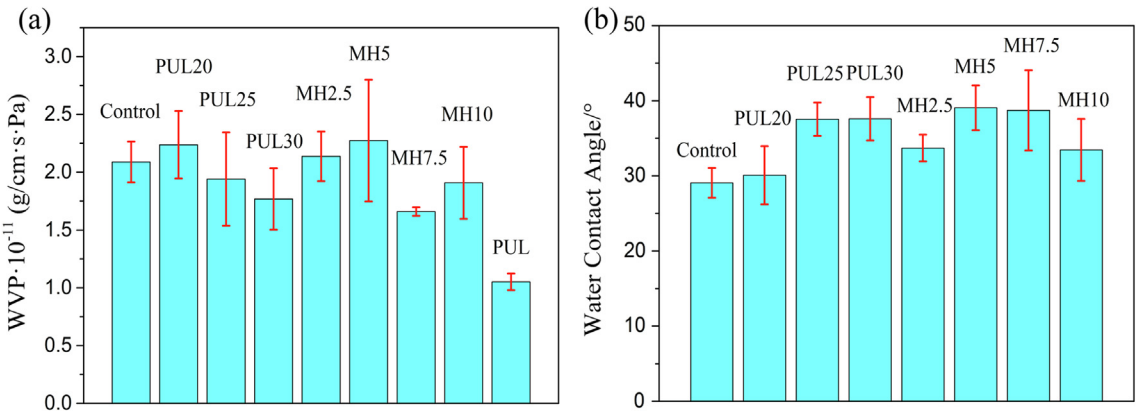

Fig. 5 (a) WVP and (b) WCA of ternary blend films.

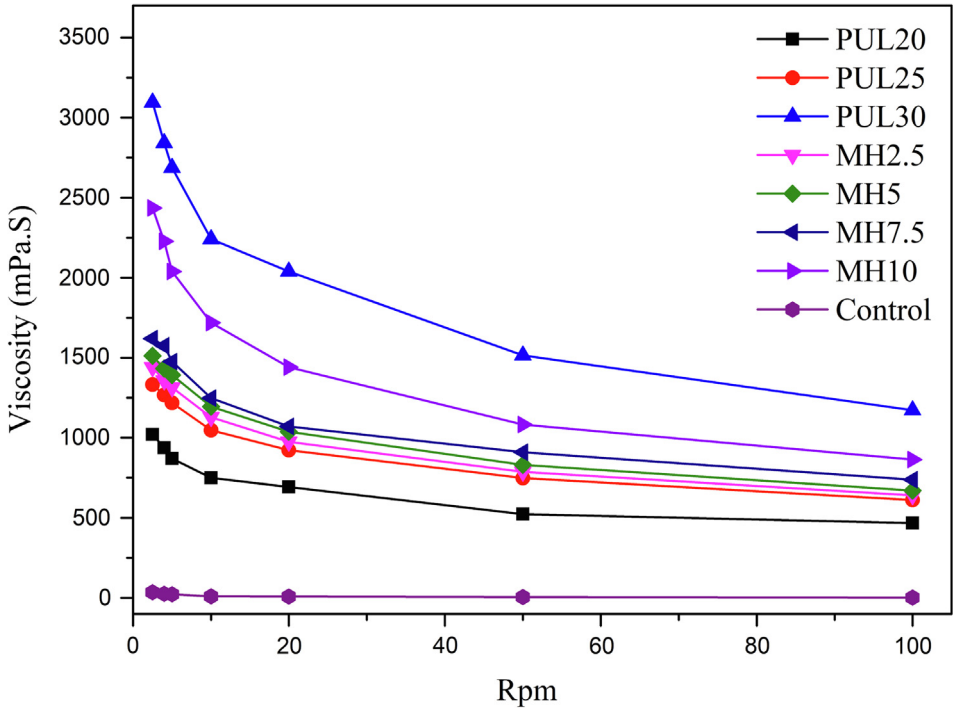

Fig. 6 Viscosity of ternary blend films.

forming solutions increased substantially after PUL was added. The crosslinking, expansion, unfolding and aggregation of polymer chain all can increase the viscosity of solutions (Wu et al., 2011). In sample PUL 20 and PUL 25, crosslinking contributed more on viscosity. In sample PUL 30, aggregation was more decisive, thus decrease the mechanical properties. The typical shear thinning behavior of non-Newtonian fluids can be observed at low rpm. This phenomenon was ascribed to the fact that rate of intermolecular junctions was disrupted faster than the reformation as the shear rate increased and the orientation of polymer chains along the stream line of the flow (Chang et al., 2021, Kaczmarek, et al., 2020). The addition of MH also increased the viscosity due to the filler van der Waals interaction (Tang et al., 2018), but far less than the effect of PUL on the blend.

3.9. Antimicrobial activity

The diameter of inhibition zones against *S. aureus* and *E. coli* are plotted in Fig. 7**.** A concise schematic diagram of experiment is presented in Fig. 8. The films were more sensitive to *S. aureus* and began to exhibit antibacterial activity at a concentration of 5 % MH, lower than against *E. coli*. Furthermore, the inhibition zones for *S. aureus* were larger than *E. coli* indicated stronger inhibiting effect on *S. aureus* for the reason of good barrier effect from lipopolysaccharide layer around the cell wall of Gram-negative bacteria (Benavides, et al., 2012). Several factors, such as molecular conformation, hydrophobicity, solubility, sugar moiety and the type of sugar in the chemical backbone, all could take effect on antibacterial activity of flavonoids (Iranshahi et al., 2015). Flavonoids

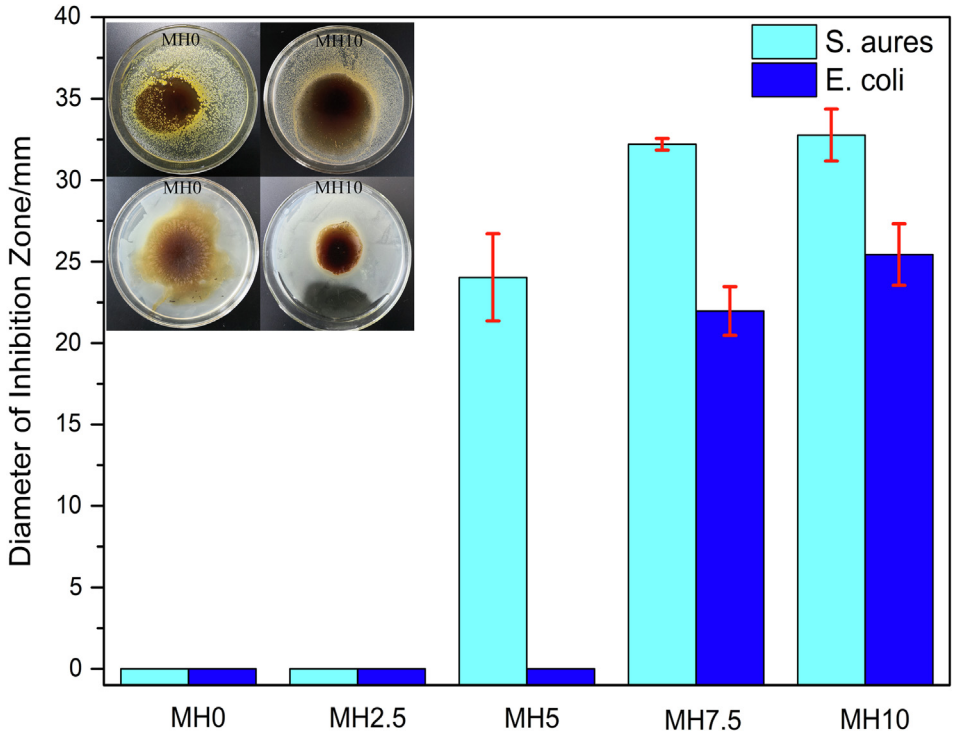

Fig. 7 The diameter of inhibition zones.

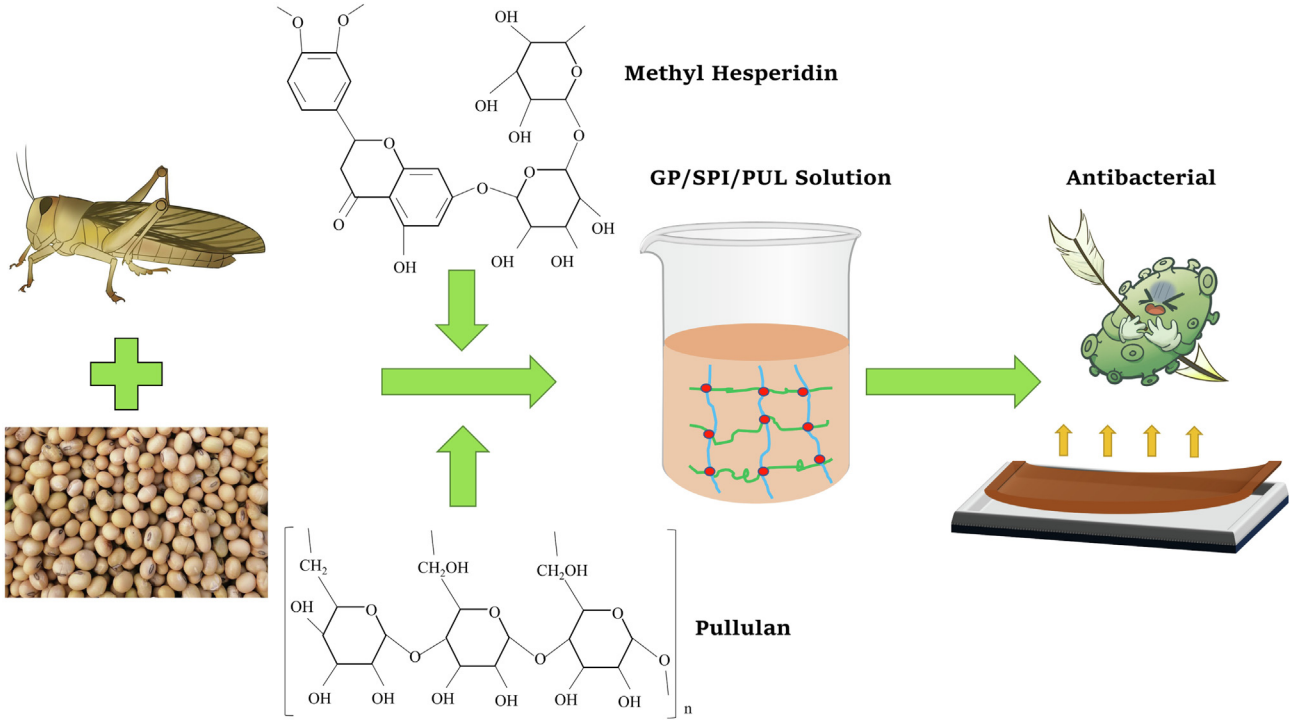

Fig. 8 The schematic diagram of experiment.

mainly interfere with energetic metabolism and cytoplasmic membrane function, inhibit nucleic acid and cell membrane synthesis to achieve antibacterial function (Xie et al., 2015). Common extracts (hesperidin, rutin, naringin) from *citrus* peel are very similar in structure and have huge amount of hydroxyl groups, adhering to the cell membrane by hydrogen bonding and destroy its structure or produce delocalized electrons to affect the normal function of the cell (Chibane et al., 2018).

Gyawali et al., (2014) also mentioned the effect of hydroxyl groups' position and number of double bonds on antibacterial activity. Pauli et al., (1987) confirmed the powerful antifungal effects after attached alkyl or methoxy groups.

4. Conclusion

The GP/SPI/PUL ternary blend composites showed good compatibility and the section morphology was more like a two-phase distributed sea-island structure. 25 % PUL can increase the TS of ternary composites from 3.4 MPa to 7.0 MPa on the premise of keeping EAB stable. Excessive MH reduced crystallinity and impaired the mechanical properties of ternary composites, especially the decrease of EAB. The barrier properties and hydrophobicity of film increased slightly after modification. In addition, ternary composites exhibited lower initial decomposition temperatures and glass transition temperatures, damaging the thermal stability. The final antimicrobial test showed good bacteriostatic properties on *E. coli* and *S. aureus* of ternary blend with addition of MH. This study proved a great application prospect of edible insect protein in active packaging. As for the GP/SPI/PUL composites, there is still large room for improvement on the water resistance and barrier properties.

CRediT authorship contribution statement

Zisen Zhang: Conceptualization, Methodology, Investigation, Data curation, Writing – original draft. **Fang Changqing:** Resources, Project administration, Supervision, Funding acquisition. **Wei Zhang:** Methodology, Resources. **Wanqing Lei:** Validation, Writing – review & editing. **Dong Wang:** Validation, Supervision. **Xing Zhou:** Methodology, Supervision.

Acknowledgements

This work was supported by the National Key Research and Development Program of China (No. 2021YFD1600402), Shaanxi Provincial Department of Education Collaborative Innovation Center Project (20JY052), Scientific Research Project of Shannxi Provincial Education Department (22JK0472), Xi'an Science and Technology Plan Project (22GXFW0073), Opening Project of Shanxi Key Laboratory of Advanced Manufacturing Technology (No. XJZZ202001).

References

Aceituno-Medina, M., Mendoza, S., Lagaron, J.M., López-Rubio, A., 2013. Development and characterization of food-grade electrospun fibers from amaranth protein and pullulan blends. Food Res. Int. 54 (1), 667–674.

Ahmed, S., Liu, F., Khin, M.N., Yokoyama, W.H., Zhong, F., 2020. Improvement of the water resistance and ductility of gelatin film by zein. Food Hydrocolloids 105.

Ahmed, J., Mulla, M.Z., Arfat, Y.A., 2016. Thermo-mechanical, structural characterization and antibacterial performance of solvent casted polylactide/cinnamon oil composite films. Food Control 69, 196–204.

Alexandre, E.M.C., Lourenço, R.V., Bittante, A.M.Q.B., Moraes, I.C. F., Sobral, P.J.D., 2016. Gelatin-based films reinforced with montmorillonite and activated with nanoemulsion of ginger essential oil for food packaging applications. Food Packag. Shelf Life 10, 87–96.

Al-Hassan, A.A., Norziah, M.H., 2012. Starch-gelatin edible films: Water vapor permeability and mechanical properties as affected by plasticizers. Food Hydrocoll. 26 (1), 108–117.

Amjadi, S., Gholizadeh, S., Ebrahimi, A., Almasi, H., Hamishehkar, H., Taheri, R.A., 2022. Development and characterization of the carvone-loaded zein/pullulan hybrid electrospun nanofibers for food and medical applications. Ind. Crop. Prod. 183, 114964.

Anankware, J.P., Roberts, B.J., Cheseto, X., Osuga, I., Savolainen, V., Collins, C.M., 2021. The Nutritional Profiles of Five Important Edible Insect Species From West Africa-An Analytical and Literature Synthesis. Front. Nutr. 8, 792941.

Azeredo, H.M.C., Waldron, K.W., 2016. Crosslinking in polysaccharide and protein films and coatings for food contact-A review. Trends Food Sci. Technol. 52, 109–122.

Barbi, S., Messori, M., Manfredini, T., Pini, M., Montorsi, M., 2019. Rational design and characterization of bioplastics from *Hermetia illucens* prepupae proteins. Biopolymers 110 (5), e23250.

Benavides, S., Villalobos-Carvajal, R., Reyes, J.E., 2012. Physical, mechanical and antibacterial properties of alginate film: Effect of the crosslinking degree and oregano essential oil concentration. J. Food Eng. 110 (2), 232–239.

Cao, L., Liu, W., Wang, L., 2018. Developing a green and edible film from Cassia gum: the effects of glycerol and sorbitol. J. Clean. Prod. 175, 276–282.

Chang, X., Hou, Y., Liu, Q., Hu, Z., Xie, Q., Shan, Y., Li, G., Ding, S., 2021. Physicochemical and antimicrobial properties of chitosan composite films incorporated with glycerol monolaurate and nano-TiO_2. Food Hydrocoll. 119, 106846.

Chibane, L.B., Degraeve, P., Ferhout, H., Bouajila, J., Oulahal, N., 2019. Plant antimicrobial polyphenols as potential natural food preservatives. J. Sci. Food Agric. 99 (7), 1457–1474.

Ciannamea, E.M., Stefani, P.M., Ruseckaite, R.A., 2014. Physical and mechanical properties of compression molded and solution casting soybean protein concentrate based films. Food Hydrocoll. 38, 193–204.

Clarkson, C., Mirosa, M., Birch, J., 2018. Potential of extracted locusta migratoria protein fractions as value-added ingredients. Insects 9 (1), 20.

Friesen, K., Chang, C., Nickerson, M., 2015. Incorporation of phenolic compounds, rutin and epicatechin, into soy protein isolate films: mechanical, barrier and cross-linking properties. Food Chem. 172, 18–23.

Gao, Y., Mehta, K., 2001. Interchain disulfide bonds promote protein cross-linking during protein folding. J. Biochem. 129 (1), 179–183.

Govorushko, S., 2019. Global status of insects as food and feed source: a review. Trends Food Sci. Technol. 91, 436–445.

Gyawali, R., Ibrahim, S.A., 2014. Natural products as antimicrobial agents. Food Control 46, 412–429.

Haber, M., Mishyna, M., Itzhak Martinez, J.J., Benjamin, O., 2019. The influence of grasshopper (*Schistocerca gregaria*) powder enrichment on bread nutritional and sensorial properties. LWT Food Sci. Technol. 115, 108395.

Haghighatpanah, N., Omar-Aziz, M., Gharaghani, M., Khodaiyan, F., Hosseini, S.S., Kennedy, J.F., 2022. Effect of mung bean protein isolate/pullulan films containing marjoram (*Origanum majorana* L.) essential oil on chemical and microbial properties of minced beef meat. Int. J. Biol. Macromol. 201, 318–329.

Haghighatpanah, N., Mirzaee, H., Khodaiyan, F., Kennedy, J.F., Aghakhani, A., Hosseini, S.S., Jahanbin, K., 2020. Optimization and characterization of pullulan produced by a newly identified strain of Aureobasidium pullulans. Int. J. Biol. Macromol. 152, 305–313.

Haghighi, H., Biard, S., Bigi, F., De Leo, R., Bedin, E., Pfeifer, F., Siesler, H.W., Licciardello, F., Pulvirenti, A., 2019. Comprehensive characterization of active chitosan-gelatin blend films enriched with different essential oils. Food Hydrocoll. 95, 33–42.

Han, Y., Yu, M., Wang, L., 2018. Preparation and characterization of antioxidant soy protein isolate films incorporating licorice residue extract. Food Hydrocolloids 75, 13–21.

Hassannia-Kolaee, M., Khodaiyan, F., Pourahmad, R., Shahabi-Ghahfarrokhi, I., 2016. Development of ecofriendly bionanocom-

posite: Whey protein isolate/pullulan films with nano-SiO_2. Int. J. Biol. Macromol. 86, 139–144.
He, X., Luzi, F., Hao, X., Yang, W., Torre, L., Xiao, Z., Xie, Y., Puglia, D., 2019. Thermal, antioxidant and swelling behaviour of transparent polyvinyl (alcohol) films in presence of hydrophobic citric acid-modified lignin nanoparticles. Int. J. Biol. Macromol. 127, 665–676.
Hosseini, S.F., Rezaei, M., Zandi, M., Farahmandghavi, F., 2015. Bio-based composite edible films containing *Origanum vulgare* L. essential oil. Ind. Crop. Prod. 67, 403–413.
Huang, T., Tu, Z., Shangguang, X., Sha, X., Wang, H., Zhang, L., Bansal, N., 2019. Fish gelatin modifications: A comprehensive review. Trends Food Sci. Technol. 86, 260–269.
Hurwitz, G., Guillen, G.R., Hoek, E.M.V., 2010. Probing polyamide membrane surface charge, zeta potential, wettability, and hydrophilicity with contact angle measurements. J. Membr. Sci. 349 (1–2), 349–357.
Iranshahi, M., Rezaee, R., Parhiz, H., Roohbakhsh, A., Soltani, F., 2015. Protective effects of flavonoids against microbes and toxins: The cases of hesperidin and hesperetin. Life Sci. 137, 125–132.
Jia, X.W., Qin, Z.Y., Xu, J.X., Kong, B.H., Liu, Q., Wang, H., 2020. Preparation and characterization of pea protein isolate-pullulan blend electrospun nanofiber films. Int. J. Biol. Macromol. 157, 641–647.
Kaczmarek, B., Lewandowska, K., Sionkowska, A., 2020. Modification of collagen properties with ferulic acid. Materials 13 (15), 3419.
Karim, M.R., Lee, H.W., Kim, R., Ji, B.C., Cho, J.W., Son, T.W., Oh, W., Yeum, J.H., 2009. Preparation and characterization of electrospun pullulan/montmorillonite nanofiber mats in aqueous solution. Carbohydr. Polym. 78 (2), 336–342.
Katashima, T., 2021. Rheological studies on polymer networks with static and dynamic crosslinks. Polym. J. 53 (10), 1073–1082.
Khadidja, L., Asma, C., Mahmoud, B., Mereim, E., 2017. Alginate/gelatin crosslinked system through Maillard reaction: preparation, characterization and biological properties. Polym. Bull. 74, 4899–4919.
Khanzadi, M., Jafari, S.M., Mirzaei, H., Chegini, F.K., Maghsoudlou, Y., Dehnad, D., 2015. Physical and mechanical properties in biodegradable films of whey protein Concentrate-pullulan by application of beeswax. Carbohydr. Polym. 118, 24–29.
Lee, J.H., Jeong, D., Kanmani, P., 2019. Study on physical and mechanical properties of the biopolymer/silver based active nanocomposite films with antimicrobial activity. Carbohydr. Polym. 224, 115159.
Li, Y., Bai, Y., Huang, J., Yuan, C., Ding, T., Liu, D., Hu, Y., 2020. Airglow discharge plasma treatment affects the surface structure and physical properties of zein films. J. Food Eng., 273, 109813. J. Food Eng., 313, 110762.
Lian, H., Shi, J., Zhang, X., Peng, Y., 2020. Effect of the added polysaccharide on the release of thyme essential oil and structure properties of chitosan based film. Food Packag. Shelf Life 23, 100467.
Luo, Q., Hossen, M. A., Zeng., Y., Dai, J., Li, S., Qin, W., Liu, Y., 2022. Gelatin-based composite films and their application in food packaging: A review.
Lv, L., Huang, Q., Ding, W., Xiao, X., Zhang, H., Xiong, L., 2019. Fish gelatin: The novel potential applications. J. Funct. Foods 63, 103581.
Mathew, S., Abraham, T.E., 2007. Characterisation of ferulic acid incorporated starch-chitosan blend films. Food Hydrocoll. 22 (5), 826–835.
McKay, S., Sawant, P., Fehlberg, J., Almenar, E., 2021. Antimicrobial activity of orange juice processing waste in powder form and its suitability to produce antimicrobial packaging. Waste Manag. 120, 230–239.
Moghadam, M., Salami, M., Mohammadian, M., Khodadadi, M., Emam-Djomeh, Z., 2020. Development of antioxidant edible films based on mung bean protein enriched with pomegranate peel. Food Hydrocoll. 104, 105735.
Mohammadi, M., Mirabzadeh, S., Shahvalizadeh, R., Hamishehkar, H., 2020. Development of novel active packaging films based on whey protein isolate incorporated with chitosan nanofiber and nano-formulated cinnamon oil. Int. J. Biol. Macromol. 149, 11–20.
Moradi, S., Yeganeh, J.K., 2020. Highly toughened poly(lactic acid) (PLA) prepared through melt blending with ethylene-co-vinyl acetate (EVA) copolymer and simultaneous addition of hydrophilic silica nanoparticles and block copolymer compatibilizer. Polym. Test. 91, 106735.
Narasagoudr, S.S., Hegde, V.G., Chougale, R.B., Masti, S.P., Vootla, S., Malabadi, R.B., 2020. Physico-chemical and functional properties of rutin induced chitosan/poly (vinyl alcohol) bioactive films for food packaging applications. Food Hydrocolloids 109.
Nuvoli, D., Montevecchi, G., Lovato, F., Masino, F., van der Borght, M., Messori, M., Antonelli, A., 2021. Protein films from black soldier fly (*Hermetia illucens*, Diptera: Stratiomyidae) prepupae: effect of protein solubility and mild crosslinking. J. Sci. Food Agric. 101 (11), 4506–4513.
Omrani-Fard, H., Abbaspour-Fard, M.H., Khojastehpour, M., Dashti, A., 2020. Gelatin/Whey protein- potato flour bioplastics: fabrication and evaluation. J. Polym. Environ. 28 (9), 2029–2038.
Pauli, A., Knobloch, K., 1987. Inhibitory effects of essential oil components on growth of food-contaminating fungi. Z Lebensm Unters Forsch 185 (1), 10–13.
Pinho-Ribeiro, F.A., Hohmann, M.S.N., Borghi, S.M., Zarpelon, A. C., Guazelli, C.F.S., Manchope, M.F., Casagrande, R., Verri Jr., W.A., 2015. Protective effects of the flavonoid hesperidin methyl chalcone in inflammation and pain in mice: Role of TRPV1, oxidative stress, cytokines and NF-κB. Chem. Biol. Interact. 228, 88–99.
Prasad, P., Guru, G.S., Shivakumar, H.R., Rai, K.S., 2008. Miscibility, thermal, and mechanical studies of hydroxypropyl methylcellulose/pullulan blends. J. Appl. Polym. Sci. 110 (1), 444–452.
Prodpran, T., Benjakul, S., Phatcharat, S., 2012. Effect of phenolic compounds on protein cross-linking and properties of film from fish myofibrillar protein. Int. J. Biol. Macromol. 51, 774–782.
Qian, X., Gu, Y., Sun, B., Ma, S., Tian, X., Wang, X., 2022. Improvement in quality of fast-frozen steamed bread by different gluten content and glutenin/gliadin ratio and its mechanism. LWT-Food Sci. Technol. 153, 112562.
Qin, Z., Jia, X., Liu, Q., Kong, B., Wang, H., 2019. Fast dissolving oral films for drug delivery prepared from chitosan/pullulan electrospinning nanofibers. Int. J. Biol. Macromol. 137, 224–231.
Qin, Z., Jia, X., Liu, Q., Kong, B., Wang, H., 2020. Enhancing physical properties of chitosan/pullulan electrospinning nanofibers via green crosslinking strategies. Carbohydr. Polym. 247, 116734.
Quéré, D., 2008. Wetting and roughness. Annual Rev. Mater. Res. 38, 71–99.
Ramos, Ó.L., Reinas, I., Silva, S.I., Fernandes, J.C., Cerqueira, M.A., Pereira, R.N., Vicente, A.A., Poças, M.F., Pintado, M.E., Malcata, F.X., 2013. Effect of whey protein purity and glycerol content upon physical properties of edible films manufactured therefrom. Food Hydrocoll. 30 (1), 110–122.
Rastin, H., Jafari, S.H., Saeb, M.R., Khonakdar, H.A., Wagenknecht, U., Heinrich, G., 2014. On the reliability of existing theoretical models in anticipating type of morphology and domain size in HDPE/PA-6/EVOH ternary blends. Eur. Polym. J. 53, 1–12.
Reddy, R., Jiang, Q., Aramwit, P., Reddy, N., 2021. Litter to Leaf: The Unexplored Potential of Silk Byproducts. Trends Biotechnol. 39 (7), 706–718.
Ren, J., Fu, H., Ren, T., Yuan, W., 2009. Preparation, characterization and properties of binary and ternary blends with thermoplastic starch, poly(lactic acid) and poly(butylene adipate-co-terephthalate). Carbohydr. Polym. 77 (3), 576–582.
Ribeiro, A.C.B., Cunha, A.P., da Silva, L.M.R., Mattos, A.L.A., de Brito, E., de Souza Filho, M.S.M., de Azeredo, H.M.C., Ricardo, N.M.P.S., 2021. From mango by-product to food packaging:

Pectin-phenolic antioxidant films from mango peels. Int. J. Biol. Macromol. 193 (Part B), 1138–1150.
Roy, S., Rhim, J.W., 2021. Effect of chitosan modified halloysite on the physical and functional properties of pullulan/chitosan biofilm integrated with rutin. Appl. Clay Sci. 211, 106205.
Saeb, M.R., Khonakdar, H.A., Razban, M., Jafari, S.H., Garmabi, H., Wagenknecht, U., 2012. Morphology prediction in HDPE/PA-6/EVOH ternary blends: Defining the role of elasticity ratio. Macromol. Chem. Phys. 213 (17), 1791–1802.
Shariatpanahi, H., Nazokdast, H., Hemmati, M., 2003. Dispersed phase particle size in polymer blends: Interfacial and rheological effects. J. Elastomers Plast. 35 (2), 115–131.
Shojaee-Aliabadi, S., Hosseini, H., Mohammadifar, M.A., Mohammadi, A., Ghasemlou, M., Ojagh, S.M., Hosseini, S.M., Khaksar, R., 2013. Characterization of antioxidant-antimicrobial κ-carrageenan films containing *Satureja hortensis* essential oil. Int. J. Biol. Macromol. 52, 116–124.
Singh, R.S., Kaur, N., Kennedy, J.F., 2015. Pullulan and pullulan derivatives as promising biomolecules for drug. Carbohydr. Polym. 123, 190–207.
Sui, G., Wang, K., Xu, S., Liu, Z., Zhang, Q., Du, R., Fu, Q., 2019. The combined effect of reactive and high-shear extrusion on the phase morphologies and properties of PLA/OBC/EGMA ternary blends. Polymer 169, 66–73.
Tabasum, S., Noreen, A., Maqsood, M.F., Umar, H., Akram, N., Nazli, Z.I.H., Chatha, S.A.S., Zia, K.M., 2018. A review on versatile applications of blends and composites of pullulan with natural and synthetic polymers. Int. J. Biol. Macromol. 120, 603–632.
Tang, Y., Zhang, X., Zhao, R., Guo, D., Zhang, J., 2018. Preparation and properties of chitosan/guar gum/nanocrystalline cellulose nanocomposite films. Carbohydr. Polym. 197, 128–136.
Tong, X., Cao, J., Tian, T., Lyu, B., Miao, L., Lian, Z., Cui, W., Liu, S., Wang, H., Jiang, L., 2022. Changes in structure, rheological property and antioxidant activity of soy protein isolate fibrils by ultrasound pretreatment and EGCG. Food Hydrocoll. 122, 107084.
Tong, Q., Xiao, Q., Lim, T.K., 2008. Preparation and properties of pullulan–alginate–carboxymethylcellulose blend films. Food Res. Int. 41, 1007–1014.
Vinodhini, P.A., Sangeetha, K., Gomathi, T., Sudha, P.N., Venkatesan, J., Anil, S., 2017. FTIR, XRD and DSC studies of nanochitosan, cellulose acetate and polyethylene glycol blend ultrafiltration membranes. Int. J. Biol. Macromol. 104 (Part B), 1721–1729.
Wang, Z., Ding, Z., Li, Z., Ding, Y., Jiang, F., Liu, J., 2021. Antioxidant and antibacterial study of 10 flavonoids revealed rutin as a potential antibiofilm agent in *Klebsiella pneumoniae* strains isolated from hospitalized patients. Microb. Pathog. 159, 105121.
Wu, X., Liu, Q., Luo, Y., Murad, M.S., Zhu, L., Mu, G., 2020. Improved packing performance and structure-stability of casein edible films by dielectric barrier discharges (DBD) cold plasma. Food Packag. Shelf Life 24, 100471.
Wu, L., Wen, Q., Yang, X., Xu, M., Yin, S., 2011. Wettability, surface microstructure and mechanical properties of films based on phosphorus oxychloride-treated zein. J. Sci. Food Agric. 91 (7), 1222–1229.
Wu, J., Zhong, F., Li, Y., Shoemaker, C.F., Xia, W., 2013. Preparation and characterization of pullulan-chitosan and pullulan-carboxymethyl chitosan blended films. Food Hydrocoll. 30 (1), 82–91.
Xia, C., Zhang, S., Shi, S.Q., Cai, L., Garcia, A.C., Rizvi, H.R., D'Souza, N.A., 2016. Property enhancement of soy protein isolate-based films by introducing POSS. Int. J. Biol. Macromol. 82, 168–173.
Xiao, Q., Lu, K., Tong, Q., Liu, C., 2015. Barrier properties and microstructure of pullulan–alginate-based films. J. Food Process Eng. 38 (2), 155–161.
Xie, Y., Yang, W., Tang, F., Chen, X., Ren, L., 2015. Antibacterial activities of flavonoids: structure-activity relationship and mechanism. Curr. Med. Chem. 22 (1), 132–149.
Yang, Y., Zheng, S., Liu, Q., Kong, B., Wang, H., 2020. Fabrication and characterization of cinnamaldehyde loaded polysaccharide composite nanofiber film as potential antimicrobial packaging material. Food Packag. Shelf Life 26, 100600.
Zhang, Z., Fang, C., Liu, D., Zhou, X., Wang, D., Zhang, W., 2022a. Preparation and characterization of the protein edible film extracted from the migratory locust (*Locusta migratoria*). Food Packag. Shelf Life 33, 100899.
Zhang, L., Huang, C., Xu, Y., Huang, H., Zhao, H., Wang, J., Wang, S., 2020. Synthesis and characterization of antibacterial polylactic acid film incorporated with cinnamaldehyde inclusions for fruit packaging. Int. J. Biol. Macromol. 164, 4547–4555.
Zhang, Z., Zhou, X., Fang, C., Wang, D., 2022b. Characterization of the antimicrobial edible film based on grasshopper protein/soy protein isolate/cinnamaldehyde blend crosslinked with xylose. Front. Nutr. 9, 796356.
Zhao, Z., Xiong, X., Zhou, H., Xiao, Q., 2019. Effect of lactoferrin on physicochemical properties and microstructure of pullulan-based edible films. J. Sci. Food Agric. 99 (8), 4150–4157.
Zhu, G., Sheng, L., Tong, Q., 2014. Preparation and characterization of carboxymethyl-gellan and pullulan blend films. Food Hydrocoll. 35, 341–347.
Zielińska, E., Baraniak, B., Karaś, M., Rybczyńska, K., Jakubczyk, A., 2015. Selected species of edible insects as a source of nutrient composition. Food Res. Int. 77 (3), 460–466.